

OPTICAL/INFRARED OBSERVATIONS OF THE ANOMALOUS X-RAY PULSAR 1E 1048.1–5937 DURING ITS 2007 X-RAY FLARE

ZHONGXIANG WANG¹, CEES BASSA¹, VICTORIA M. KASPI¹, JULIA J. BRYANT², AND NIDIA MORRELL³

Draft version February 14, 2008

ABSTRACT

We report on optical and infrared observations of the anomalous X-ray pulsar (AXP) 1E 1048.1–5937, made during its ongoing X-ray flare which started in 2007 March. We detected the source in the optical *I* and near-infrared *K_s* bands in two ground-based observations and obtained deep flux upper limits from four observations, including one with the *Spitzer Space Telescope* at 4.5 and 8.0 μm . The detections indicate that the source was approximately 1.3–1.6 magnitudes brighter than in 2003–2006, when it was at the tail of a previous similar X-ray flare. Similar related flux variations have been seen in two other AXPs during their X-ray outbursts, suggesting common behavior for large X-ray flux variation events in AXPs. The *Spitzer* flux limits are sufficiently deep that we can exclude mid-infrared emission similar to that from the AXP 4U 0142+61, which has been interpreted as arising from a dust disk around the AXP. The optical/near-infrared emission from 1E 1048.1–5937 probably has a magnetospheric origin. The similarity in the flux spectra of 1E 1048.1–5937 and 4U 0142+61 challenges the dust disk model proposed for the latter.

Subject headings: stars: neutron — pulsars: individual (1E 1048.1–5937) — infrared: stars — X-rays: stars

1. INTRODUCTION

Supported by extensive observational studies over the past few years, it is generally believed that anomalous X-ray pulsars (AXPs) are magnetars—young neutron stars possessing ultra-high $\sim 10^{14}$ G magnetic fields. While AXPs are primarily known as X-ray sources, exhibiting a variety of variability behavior related to their magnetar nature (Woods & Thompson 2006; Kaspi 2007), we now know that 5 of 10 identified AXPs—4U 0142+61, 1E 1048.1–5937, 1RXS J170849–400910, XTE J1810–197, and 1E 2259+586—are bright at near-infrared (NIR) wavelengths (Woods & Thompson 2006; McGill AXP online catalog⁴). Among them, the AXP 4U 0142+61 is detected from optical to mid-infrared (MIR) wavelengths, indicating a spectral energy distribution (SED) that can be described by a two-component model: one a power-law spectrum over optical *VRI* and NIR *J* bands, presumably arising from the magnetosphere, and one thermal blackbody-like over the 2.2–8 μm range (Wang et al. 2006), arising from a debris disk. The discovery of such an optical/IR SED from the AXP was unexpected, and the two-component model remains controversial (e.g., Durant & van Kerkwijk 2006b). Ideally, in order to understand the optical/IR emission mechanism for AXPs and in particular determine whether the IR emission from 4U 0142+61 is unusual or generic among AXPs, SEDs of other AXPs must be observed. However, most known AXPs are highly extincted in the optical range and often extremely faint in the IR.

Among the known AXPs, 1E 1048.1–5937 is peculiar in that it has exhibited two long-term X-ray flares (Gavril & Kaspi 2004; Tam et al. 2008) which have not

been seen from other AXPs thus far. Monitored with the *Rossi X-ray Timing Explorer (RXTE)*, the first flare was found to start in 2002 April and lasted approximately two years. At the beginning of the flare, the NIR counterpart was discovered (Wang & Chakrabarty 2002), and in observations more than a year later, the counterpart was found to be approximately 2 magnitudes dimmer in *JK_s* (Durant & van Kerkwijk 2005), suggesting large flux variations associated with the flare. Such flaring events thus provide an opportunity to study optical/IR emission from an AXP other than 4U 0142+61. In addition, during their X-ray outbursts, the AXPs 1E 2259+586 and XTE J1810–197 both exhibited related NIR brightening. In the first source, its NIR and X-ray flux changes were correlated (Tam et al. 2004) while in the latter, its NIR flux did not exactly follow the decline of the X-ray flux (Rea et al. 2004; Camilo et al. 2007). Optical/IR observations of 1E 1048.1–5937 during another X-ray flare would allow us to verify if the source exhibits similar emission behavior.

For these reasons, after a second flare started on 2007 March 24 (Dib et al. 2007), we made multi-wavelength observations of 1E 1048.1–5937 with large ground-based telescopes and the *Spitzer Space Telescope*. In this paper, we report on our optical/IR observations during this ongoing X-ray flare.

2. OBSERVATIONS AND DATA REDUCTION

2.1. Ground-Based Observations

2.1.1. NIR Imaging

On 2007 April 04, we observed the 1E 1048.1–5937 field in *K_s* band using Persson’s Auxiliary Nasmyth Infrared Camera (PANIC; Martini et al. 2004) on the 6.5-m Baade Magellan Telescope at Las Campanas Observatory in Chile. The detector is a Rockwell Hawaii 1024×1024 HgCdTe array, having a field of view (FOV) of $2' \times 2'$ and a pixel scale of 0.125"/pixel. The total on-source exposure time was 15 min. During the exposure, the telescope

¹ Department of Physics, McGill University, QC H3A 2T8, Canada

² School of Physics, University of Sydney, NSW 2006, Australia

³ Las Campanas Observatory, Observatories of the Carnegie Institution of Washington, La Serena, Chile

⁴ www.physics.mcgill.ca/pulsar/magnetar/main.html

was dithered in a 3×3 grid with offsets of $10''$ to obtain a measurement of the sky background. The observing conditions were good, with $0.5''$ seeing in K_s .

On 2007 May 08, we observed the target field in the same band with the same telescope and camera. The total on-source time was 18 min, and the same observing strategy was used. During the exposure, the conditions were not stable, with K_s seeing rapidly changing between $0.6''$ and $0.8''$.

2.1.2. Optical Imaging

We observed the target field in the optical bands using the 8.2-m Very Large Telescope (VLT; ANTU) at the European Southern Observatory (ESO) and the 8-m Gemini South Telescope at the Gemini Observatory. Both telescopes are located in Chile.

The VLT observation was made on 2007 May 07, the same night that the second Magellan NIR image was obtained. The instrument used was the Focal Reducer and low dispersion Spectrograph (FORS2; Appenzeller et al. 1998), which consists of two $2k\times 4k$ MIT CCDs and has a FOV of $6.8'\times 6.8'$. The CCD detectors were 2×2 binned, having a pixel scale of $0.25''/\text{pixel}$. We obtained 15 3-min I -band images of the field, resulting in a 45 min total exposure. The telescope was dithered in a 3×5 grid, with offsets of $5''\times 2.5''$. The conditions were excellent, with $0.5''$ seeing.

The Gemini imaging observations were made on 2007 June 24 and July 15. The instrument was Gemini Multi-Object Spectrograph (GMOS; Hook et al. 2004). The detector array of GMOS consists of three 2048×4608 EEV CCDs. The pixel scale is $0.073''/\text{pixel}$, while we used a detector binning of 2 pixels for the observations. In the first observation, we obtained 8 r' and 5 i' images, with exposure times of 5 and 3 min, respectively. The telescope was dithered for the exposures, with offsets of $10''$. The seeing was approximately $0.9''$ during the observations. In the latter observation, we obtained 16 5-min r' and 4 3-min i' images, with the same observing strategy. The seeing was approximately $0.8''$.

2.1.3. Data Reduction

We used the IRAF data analysis package for data reduction. The images were bias-subtracted and flat-fielded. In addition, because the Gemini GMOS detectors have significant fringing in i' band, a fringe frame provided by the Gemini Observatory was used for subtraction of the fringes in our i' images. From each set of dithered images in one observation, a sky image was made by filtering out stars. The sky image was subtracted from the set of images, and then the sky-subtracted images were shifted and combined into one final image of the target field. A summary of the images we obtained is given in Table 1.

2.2. Spitzer 4.5/8.0 μm Imaging

We also observed 1E 1048.1–5937 on 2007 August 10 with the *Spitzer Space Telescope*. The imaging instrument used was the Infrared Array Camera (IRAC; Fazio et al. 2004). It operates in four channels at 3.6, 4.5, 5.8, and $8.0\ \mu\text{m}$, while two adjacent fields are simultaneously imaged in pairs (3.6 and $5.8\ \mu\text{m}$; 4.5 and $8.0\ \mu\text{m}$). We observed our target in the 4.5 (bandwidth $1.0\ \mu\text{m}$)

and $8.0\ \mu\text{m}$ (bandwidth $2.9\ \mu\text{m}$) channels. The detectors at the short and long wavelengths are InSb and Si:As devices, respectively, with 256×256 pixels and a plate scale of $1''.2/\text{pixel}$. The field of view (FOV) is $5''.2\times 5''.2$. The frame time was 100 s, with 96.8 and 93.6 s effective exposure time per frame for the 4.5 and $8.0\ \mu\text{m}$ data, respectively. The total exposure times in each observation were 53.2 min at $4.5\ \mu\text{m}$ and 51.5 min at $8.0\ \mu\text{m}$.

The raw image data were processed through the IRAC data pipelines (version S16.1.0) at the *Spitzer* Science Center (SSC). In the Basic Calibrated Data (BCD) pipeline, standard imaging data reductions, such as removal of the electronic bias, dark sky subtraction, flat-fielding, and linearization, are performed and individual flux-calibrated BCD frames are produced. In the post-BCD (PBCD) pipeline, radiation hits in BCD images are detected and excluded, and BCD frames are then combined into final PBCD mosaics. The details of the data reduction in the pipelines can be found in the IRAC Data Handbook (version 3.0; Reach et al. 2006).

3. RESULTS

3.1. Ground-based Observations

The counterpart to 1E 1048.1–5937 was detected in both NIR observations made on 2007 April 04 and the optical observations made on 2007 May 07. We performed PSF-fitting photometry to measure the brightness of the source. The nearby field star X5 was used for flux calibration in the K_s and I bands (Durant & van Kerkwijk 2005). The source's magnitudes were $K_s = 19.9 \pm 0.1$ and $I = 24.9 \pm 0.2$. We did not detect the source in the other observations. Using the X5 star for flux calibration (Wang & Chakrabarty 2002), we derived 3σ limiting magnitudes for the Magellan K_s and Gemini r' and i' images. The results are given in Table 1.

3.2. Spitzer/IRAC Observations

We did not detect the source in the *Spitzer* IRAC 4.5 and $8.0\ \mu\text{m}$ images, and the derived 3σ flux upper limits were 5.2 and $21.8\ \mu\text{Jy}$, respectively. The fluxes correspond to limiting magnitudes of 18.9 and 16.2 mag, for the zero magnitude fluxes of 179.7 and 64.1 Jy (Reach et al. 2005) at the *Spitzer*/IRAC 4.5 and $8.0\ \mu\text{m}$ bands, respectively. These results are also given in Table 1. The source region has been observed previously with IRAC at the same wavelength bands in 2005, with no counterpart found either (Wang et al. 2007). Comparing to the previous results, our 2007 upper limits are approximately 2 times deeper.

4. DISCUSSION

The optical/NIR counterpart of 1E 1048.1–5937 was observed a few times during 2003–2006 after the discovery of the counterpart, and the source's brightness had been low (e.g., $K_s \simeq 21.0$ – 21.5 ; see Tam et al. 2008 for details). Compared to the flux measurements, particularly those obtained in 2003 April and June when the counterpart was detected in both the optical I and NIR JK_s bands (Durant & van Kerkwijk 2005; also see Table 2), our results clearly indicate an optical/NIR brightening during the 2007 X-ray flare. Indeed, assuming $A_V = 5.4$ mag, the unabsorbed optical/NIR-to-X-ray flux ratios for the 2003 and our measurements

are nearly identical (see Figure 1). In this comparison, the unabsorbed 2–10 keV X-ray fluxes at two epochs given in Table 2 are used, and A_V is estimated from $N_H = 9.7 \times 10^{21} \text{ cm}^{-2}$ (Tam et al. 2008) by using the relation $A_V = N_H / 1.79 \times 10^{21} \text{ cm}^{-2}$ (Predehl & Schmitt 1995). Also we note that even though our second K_s measurement was an upper limit ($K_s > 20.1$), it was only 0.1 mag smaller than that obtained from a detection two days later by Israel et al. (2007). Thus in these two sets of observations, the optical/NIR and X-ray fluxes appeared to be correlated.

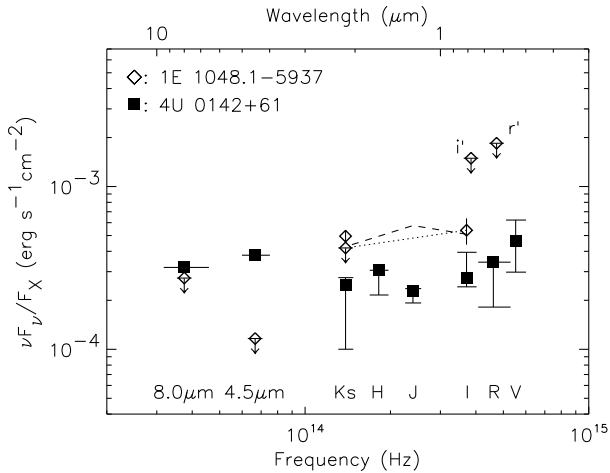


FIG. 1.— Unabsorbed optical/IR flux and flux upper limits (diamonds) of 1E 1048.1–5937 measured in 2007 April–August, normalized by the unabsorbed 2–10 keV X-ray flux obtained on 2007 April 28 (see Table 2). The dotted line indicates our two nearly simultaneous observations in the I and K_s bands, and the dashed line indicates the optical and NIR measurements obtained in 2003 April and June (Durant & van Kerkwijk 2005). For comparison, the unabsorbed optical/IR-to-X-ray flux ratios for 4U 0142+61 are also shown (squares; Durant & van Kerkwijk 2006b; Wang & Kaspi 2008), with the vertical and horizontal lengths of the bars indicating the flux variation range and effective bandwidth at each band, respectively. $A_V = 3.5$ (Durant & van Kerkwijk 2006a) is used for dereddening. The unabsorbed 2–10 keV X-ray flux used for 4U 0142+61 was $6.6 \times 10^{-11} \text{ ergs s}^{-1} \text{ cm}^{-2}$ (Gonzalez et al. 2007).

However, as shown by Tam et al. (2008), the observed NIR brightening at the beginning of the 2002 X-ray flare preceded the pulsed X-ray flux peak by ~ 2 months. If we assume that the relation between the pulsed flux F_p and total flux F_t , $F_p \propto F_t^{0.54}$ (Tam et al. 2008), is generally true for this AXP, the 2–10 keV unabsorbed total flux derived at the NIR observation time would have been $\sim 10^{-11} \text{ ergs s}^{-1} \text{ cm}^{-2}$, 3.6 times lower than the 2007 peak flux. As a result, the 2002 NIR-to-X-ray flux ratios would be approximately 6 times higher than that shown in Figure 1 (note $K_s = 19.4$ in the 2002 detection). This would indicate that the NIR and X-ray fluxes were not correlated all the time. We note that since the F_p and F_t relation is mainly based on the total flux measurements obtained during the 2007 flare and there were not such measurements for the 2002 flare, it is possible that the total flux was much larger at the start of the 2002 flare, and not reflected in the *RXTE* pulsed flux measurements. In any case, we confirm that in this AXP, the large optical/NIR flux variations were related to the X-ray flares. Similar related NIR brightening has

been seen in 1E 2259+586 and XTE J1810–197 during their X-ray outbursts (Tam et al. 2004; Camilo et al. 2007), suggesting common behavior for emission from AXPs. However for 4U 0142+61, while its X-ray flux has been relatively stable (Gonzalez et al. 2007), its optical and NIR flux was found to have large, rapid variations (Durant & van Kerkwijk 2006b). This limits the related NIR/X-ray behavior to only large X-ray flux variation events.

It is instructive to compare 1E 1048.1–5937 to 4U 0142+61, since the latter has well measured fluxes from the optical to MIR. In Figure 1, we compare the optical/IR fluxes and flux upper limits of 1E 1048.1–5937 to those of 4U 0142+61, with each set of data points normalized by the approximately contemporaneous unabsorbed 2–10 keV X-ray flux of each source. The optical VRI and NIR JHK_s fluxes for 4U 0142+61 are from Durant & van Kerkwijk (2006b; because of relatively large flux variations from the source, we show the range of the flux found in each band in the figure), the two MIR data points at 4.5 and 8.0 μm are the 2005 flux measurements in Wang & Kaspi (2008), and the unabsorbed 2–10 keV X-ray flux used is $6.6 \times 10^{-11} \text{ ergs s}^{-1} \text{ cm}^{-2}$, obtained on 2004 July 24 (Gonzalez et al. 2007). As can be seen from the figure, while the flux ratios of 1E 1048.1–5937 are roughly two times larger than those of 4U 0142+61, the deep limit at 4.5 μm from our *Spitzer* IRAC observation is approximately 3 times lower than the detection of 4U 0142+61. This strongly suggests that our target does not have similar MIR emission. This difference in the MIR is not very sensitive to uncertainties on the reddening to the two sources, since MIR emission is only weakly extinguished by the interstellar medium. The X-ray flux from 4U 0142+61 has been stable (Gonzalez et al. 2007). A possible explanation could be the non-simultaneous X-ray flux of 1E 1048.1–5937 we use for the comparison. However, *RXTE* X-ray monitoring observations of the source have indicated that the pulsed flux, which is found to trace the total flux (Tam et al. 2008), has remained stable and high during our observations (Dib et al. 2008, in preparation). In order to raise the 4.5 μm upper limit to the flux ratio of 4U 0142+61, the X-ray flux would have had to have been as low as $11 \times 10^{-12} \text{ ergs s}^{-1} \text{ cm}^{-2}$, only 40% larger than the average quiescent flux ($7.7 \times 10^{-12} \text{ ergs s}^{-1} \text{ cm}^{-2}$) of the source and approximately one third of those obtained in 2007 April (Tam et al. 2008).

The lack of MIR emission similar to that of 4U 0142+61 from 1E 1048.1–5937 seems robust. In the dust disk model proposed for 4U 0142+61 (Wang et al. 2006), the MIR flux, arising from X-ray irradiation of the disk, is proportional to the X-ray flux of the pulsar. Therefore, even though our deep 4.5 μm limit was obtained during the X-ray flare, we can exclude the existence of a similar disk around 1E 1048.1–5937. However, since a disk could be further away from the central source, deep observations at longer wavelengths are needed in order to exclude the existence of a disk more conclusively. The MIR non-detection may suggest that debris disks are not commonly found around AXPs and thus the putative disk in 4U 0142+61 is unique. Two other AXPs have also been observed by *Spitzer* with no detection; however, the derived upper limits are far above the MID-to-X-ray flux ratio of 4U 0142+61 (Wang et al.

2007).

The optical and NIR emission from 1E 1048.1–5937 probably has a magnetospheric origin, given that the flux spectrum is similar to that of 4U 0142+61 (Wang & Chakrabarty 2002; Durant & van Kerkwijk 2005). For the latter source, its optical emission is known to be pulsed at the spin period and has a pulsed fraction much higher than that in X-rays, excluding a disk origin (Kern & Martin 2002; Dhillon et al. 2005). Details of how optical and NIR emission is produced in the magnetosphere of a magnetar are not known, though possible radiation mechanisms have been suggested (e.g., Beloborodov & Thompson 2007). We note that in the disk model for 4U 0142+61 (Wang et al. 2006), the *K*-band flux primarily arises from the disk, not from the magnetosphere. Therefore, the similarity in the *K*-band-to-X-ray flux ratios for the AXPs (Durant & van Kerkwijk 2005), including 1E 1048.1–5937 as confirmed by our measurements, challenges the disk model. The *K*-band emission thus should originate from the magnetosphere, which may be supported by the fact that in the absence of X-ray variability, strong *K*-band variability is seen in 4U 0142+61

(Durant & van Kerkwijk 2006b).

We thank ESO, the Gemini Observatory, and SSC for granting us the observations. We thank F. Patat at the Users Support Department of ESO, M. Bergmann at Gemini South, and N. Silbermann from SSC for helping with the observations. We also thank R. Dib and C. Tam for sharing their unpublished results. The Gemini data were taken under the program DD-2007A-DD-10-1. The Gemini Observatory is operated by the Association of Universities for Research in Astronomy, Inc., under a cooperative agreement with the NSF on behalf of the Gemini partnership: the National Science Foundation (United States), the Science and Technology Facilities Council (United Kingdom), the National Research Council (Canada), CONICYT (Chile), the Australian Research Council (Australia), CNPq (Brazil), and CONICET (Argentina). This research was supported by NSERC via a Discovery Grant and by the FQRNT and CIFAR. VMK holds a Canada Research Chair and the Lorne Trottier Chair in Astrophysics & Cosmology, and is a R. Howard Webster Foundation Fellow of CIFAR.

REFERENCES

- Appenzeller, I. et al. 1998, *The Messenger*, 94, 1
 Beloborodov, A. M. & Thompson, C. 2007, *ApJ*, 657, 967
 Camilo, F. et al. 2007, *ApJ*, 669, 561
 Dhillon, V. S., Marsh, T. R., Hulleman, F., van Kerkwijk, M. H., Shearer, A., Littlefair, S. P., Gavriil, F. P., & Kaspi, V. M. 2005, *MNRAS*, 363, 609
 Dib, R., Kaspi, V. M., Gavriil, F. P., & Woods, P. M. 2007, *The Astronomer’s Telegram*, 1041, 1
 Durant, M. & van Kerkwijk, M. H. 2005, *ApJ*, 627, 376
 —. 2006a, *ApJ*, 650, 1082
 —. 2006b, *ApJ*, 652, 576
 Fazio, G. G. et al. 2004, *ApJS*, 154, 10
 Gavriil, F. P. & Kaspi, V. M. 2004, *ApJ*, 609, L67
 Gonzalez, M. E., Dib, R., Kaspi, V. M., Woods, P. M., Tam, C. R., & Gavriil, F. P. 2007, *ArXiv e-prints*, 708, (astro-ph/0708.2756)
 Hook, I. M., Jørgensen, I., Allington-Smith, J. R., Davies, R. L., Metcalfe, N., Murowinski, R. G., & Crampton, D. 2004, *PASP*, 116, 425
 Indebetouw, R. et al. 2005, *ApJ*, 619, 931
 Israel, G. L., Campana, S., Testa, V., Mereghetti, S., Zane, S., Rea, N., Curto, G. L., & Stella, L. 2007, *The Astronomer’s Telegram*, 1077, 1
 Kaspi, V. M. 2007, *Ap&SS*, 308, 1
 Kern, B. & Martin, C. 2002, *Nature*, 417, 527
 Martini, P., Persson, S. E., Murphy, D. C., Birk, C., Shtetman, S. A., Gunnels, S. M., & Koch, E. 2004, *Proc. SPIE*, 5492, 1653, (astro-ph/0406666)
 Predehl, P. & Schmitt, J. H. M. M. 1995, *A&A*, 293, 889
 Rea, N. et al. 2004, *A&A*, 425, L5
 Reach, W. T. et al. 2005, *PASP*, 117, 978
 Reach, W. T. et al. 2006, *Infrared Array Camera Data Handbook*, ver. 3.0 (Pasadena: Spitzer Science Center)
 Schlegel, D. J., Finkbeiner, D. P., & Davis, M. 1998, *ApJ*, 500, 525
 Tam, C. R., Gavriil, F. P., Dib, R., Kaspi, V. M., Woods, P. M., & Bassa, C. 2007, *ApJ*, in press, (arXiv:0707.2093)
 Tam, C. R., Kaspi, V. M., van Kerkwijk, M. H., & Durant, M. 2004, *ApJ*, 617, L53
 Wang, Z. & Chakrabarty, D. 2002, *ApJ*, 579, L33
 Wang, Z., Chakrabarty, D., & Kaplan, D. L. 2006, *Nature*, 440, 772
 Wang, Z. & Kaspi, V. M. 2008, *ApJ*, in press
 Wang, Z., Kaspi, V. M., & Higdson, S. J. U. 2007, *ApJ*, 665, 1292
 Woods, P. M. & Thompson, C. 2006, in *Compact Stellar X-ray Sources*, ed. W. H. G. Lewin & M. van der Klis (Cambridge: Cambridge University Press), 547–586

TABLE 1
OPTICAL/IR OBSERVATIONS OF 1E 1048.1–5937

Observation Start Time (UTC)	MJD	Telescope/Instrument	Filter	Exposure (min)	Seeing ^a (arcsec)	Magnitude ^b	νF_ν ^c /10 ⁻¹⁴ (ergs s ⁻¹ cm ⁻²)
2007-04-04 00:37	54194.0	Magellan/PANIC	K_s	15	0.54	19.9±0.1	1.8
2007-05-07 23:24	54228.0	VLT/FORS2	I	45	0.55	24.9±0.2	1.9
2007-05-08 03:15	54228.1	Magellan/PANIC	K_s	18	0.66	>20.1	<1.5
2007-06-24 01:18	54275.1	Gemini-S/GMOS	r'	40	1.0	>24.8	...
			i'	15	0.88	>24.1	...
2007-07-15 00:06	54296.0	Gemini-S/GMOS	r'	80	0.92	>25.6	<6.6
			i'	12	0.74	>24.5	<5.4
2007-08-10 10:04	54322.4	Spitzer/IRAC	4.5 μ m	53.2	...	> 18.9	<0.42
			8.0 μ m	51.5	...	> 16.2	<0.99

^a Full width at half maximum. ^b The upper limits are 3σ limiting magnitudes. ^c Flux is dereddened with $A_V = 5.4$, using the reddening laws for the optical and NIR bands given in Schlegel et al. (1998) and for the *Spitzer*/IRAC data given in Indebetouw et al. (2005).

TABLE 2
FLUX MEASUREMENTS OF 1E 1048.1–5937 USED IN THE
COMPARISON.

Epoch	Optical/NIR Magnitude	νF_ν ^b	X-ray ^a	Refs
2003 April 24	$J = 23.4$	6.6	...	1
2003 June 6	$I = 26.2$	5.9	...	1
2003 June 7	$K_s = 21.5$	4.9	...	1
2003 July 16	11.5	2
2007 April 28	36.1	2

REFERENCES. — (1) Durant & van Kerkwijk (2005); (2) Tam et al. (2008).

^a X-ray flux is phase-averaged, unabsorbed, in the energy range of 2–10 keV, and in units of 10⁻¹² ergs s⁻¹ cm⁻². ^b Dereddened flux (assuming $A_V = 5.4$; in units of 10⁻¹⁵ ergs s⁻¹ cm⁻²) obtained at the tail of the first X-ray flare.